CAUCHY – Jurnal Matematika Murni dan Aplikasi
Volume 11 (1) (2026), Pages 1202-1217
p-ISSN: 2086-0382; e-ISSN: 2477-3344

# Dynamical Analysis of a Trophic Model on Guano, Invertebrates, and Fish in Cave Ecosystems

M. Niko Axsella Ibrahim and Dian Savitri*

*Department of Mathematics, Faculty of Mathematics and Natural Sciences, Universitas Negeri Surabaya, Indonesia*

**Abstract**

This study investigates the dynamical interaction between guano biomass density ($x$), invertebrate biomass density ($y$), and fish biomass density ($z$) through a three-compartment trophic model representing a nutrient-based cave ecosystem. The analysis identifies three equilibrium points: the consumer-free equilibrium $E_0$, the predator-free equilibrium $E_1$, and the coexistence equilibrium $E_2$. Local stability analysis shows that the coexistence equilibrium is asymptotically stable, characterized by eigenvalues with negative real parts ($\lambda_1 = -0.519706$ and $\lambda_{2,3} = -0.085385 \pm 0.188169i$). Numerical simulations using the fourth–fifth order Runge–Kutta method (RK45) support these analytical results, showing trajectories that exhibit damped oscillations before converging to the steady state. Furthermore, a bifurcation analysis reveals a critical Branching Point (BP) at the predation rate $b_2 \approx 0.043956$. This threshold signifies a transcritical bifurcation where the system transitions from a predator-extinction regime to a stable coexistence regime, highlighting the sensitivity of the food web to energy transfer efficiency. These findings suggest that under the assumed parameter set, the interaction between guano nutrients, invertebrates, and fish can maintain a stable ecological balance through top-down control and nutrient-dependent dynamics.

**Keywords:** guano, cave ecosystem model, local asymptotic stability, numerical simulation, three-compartment trophic model, transcritical bifurcation.

## 1. Introduction

Cave ecosystems represent some of the most unique and extreme environments within the biosphere, fundamentally characterized by permanent aphotic zones, high microclimatic stability, and significant geographical isolation. Due to the absence of sunlight to drive phototrophic processes, these ecosystems are obligately heterotrophic and function as semi-closed systems that rely heavily on allochthonous energy subsidies from the surface environment to maintain their ecological functions [1–3]. The limitation of primary productivity within caves makes them highly sensitive systems to fluctuations in external energy inputs, where even minor changes in environmental parameters can trigger significant ecological cascades for specialized subterranean biota [4]. These enclosed and energy-limited ecological conditions cause most cave organisms to depend on periodic external nutrient sources, such as surface organic matter, animal carcasses, or bat guano deposition [1].

Among these various energy transfer mechanisms, bat guano deposition is recognized as one of the most critical nutrient sources in cave ecosystems. Guano is not merely biological waste; it serves as a reservoir of organic matter rich in nitrogen (N), phosphorus (P), and organic carbon, forming the primary foundation of nutrient cycling in subterranean environments [5]. This high

*Corresponding author. E-mail: diansavitri@unesa.ac.id

Submitted: March 11, 2026 Reviewed: April 13, 2026 Accepted: May 16, 2026
DOI: https://doi.org/10.18860/cauchy.v11i1.41524

nutrient content enables the flourishing of microbial communities and detritivorous organisms that utilize guano as a primary energy source [6]. Recent studies also indicate that guano deposits can enhance microbial diversity and influence the structure of biological communities within caves, such that guano-rich areas often harbor higher biomass diversity compared to nutrient-poor sections [7]. Furthermore, stable isotope analysis of guano can even record long-term ecological dynamics and environmental changes, making it a vital indicator in studies of cave ecology and biogeochemical cycles [8].

As a primary trophic base, guano triggers the formation of unique hierarchical food webs (*trophic cascades*) within cave ecosystems. At the first trophic level, various detritivorous and coprophagous macroinvertebrates, such as Collembola, Coleoptera, and insect larvae, utilize guano as the main energy source for their biomass growth [9]. This interaction involves not only direct consumption but also microbial decomposition processes that accelerate nutrient mineralization, thereby increasing energy availability for higher trophic level organisms. The abundance of these invertebrate biomass densities subsequently supports higher-level predators, including stygobitic cave fish and other predatory arthropods, forming a trophic network that is highly dependent on the rate of guano deposition ($R$) and the efficiency of energy transfer between trophic levels [10, 11].

Nonetheless, biomass dynamics in cave ecosystems often exhibit high complexity due to extreme dependence on a single primary energy source. Unstable guano deposition rates can cause sharp fluctuations in primary consumer biomass densities, which ultimately affect the stability of predators at higher trophic levels. Disturbances to bat colonies resulting from anthropogenic activities, surface land conversion, or global climate change have the potential to drastically reduce guano supply [12, 13]. Such conditions can trigger ecological imbalances and even increase the risk of local extinction for endemic cave species highly specialized to these energy sources. Additionally, some recent studies have shown that guano can act as a medium for the accumulation of specific microorganisms and chemical compounds that may influence decomposition processes and the health of surrounding organisms [14].

To quantitatively understand these complex interactions, mathematical modeling approaches have become essential tools for analyzing biomass dynamics in energy-limited ecosystems. Historically, three-species food chain models have been a cornerstone of mathematical biology, often used to study the emergence of complex behaviors such as limit cycles and multi-stability [15]. However, recent mathematical literature has increasingly focused on the dynamics of systems driven by external resource subsidies and non-living nutrient pools [16, 17]. The system analyzed in this study belongs to the class of resource-consumer-predator models, which are mathematically analogous to chemostat-type systems with constant nutrient inflow ($R$), a framework that remains a subject of intense analytical investigation in modern dynamical systems [16].

The mathematical novelty of this study lies in the formulation of a three-compartment trophic model that explicitly integrates a non-living organic resource (guano) as the fundamental abiotic driver ($x$), rather than a self-renewing biotic biomass with logistic growth. This structural distinction is significant; unlike standard food-chain models where the basal level is self-replicating, our approach incorporates a constant allochthonous supply ($R$) and abiotic decay ($a$), which fundamentally alters the stability landscape of the subterranean food web [18]. Specifically, this work extends the existing literature on nutrient-input models by rigorously defining the invasion boundary for top predators in extreme environments through the determination of a precise transcritical bifurcation threshold. This allows us to quantify how energy transfer efficiency and guano deposition rates interact to dictate the transition from a predator-extinction regime to a stable coexistence state, a facet often overlooked in purely biotic 3D trophic models. Through equilibrium point analysis, stability evaluation, and numerical continuation methods, this research identifies the specific mathematical conditions that allow for stable coexistence, providing a specialized framework that bridges theoretical resource-consumer dynamics with cave-specific ecological constraints.

## 2. Methods and Mathematical Model

In this study, the method employed to dissect the dynamics of the cave ecosystem is dynamical systems modeling through a system of three-dimensional nonlinear differential equations. This approach was selected to represent the hierarchical trophic interactions that rely entirely on allochthonous energy subsidies, by dividing the ecosystem components into three primary state variables: the biomass density of the guano resource ($x$), the biomass density of detritivorous invertebrates ($y$), and the biomass density of cave fish as top predators ($z$). To ensure dimensional consistency, all state variables are defined in units of mass per unit area ($mass \cdot area^{-1}$). The model formulation is built upon the assumption that the cave ecosystem is a semi-closed aphotic system, where the growth of all trophic levels is fundamentally governed by a constant guano input rate ($R$) continuously deposited by bat colonies onto the cave floor.

The dynamics of the guano resource ($x$) are assumed to decrease due to natural decomposition processes at rate $a$ and consumption by invertebrates at an interaction rate $b_1$. Accordingly, the invertebrate biomass ($y$) grows proportionally to the amount of guano consumed, dictated by a conversion efficiency factor $e_1$. However, this invertebrate biomass also experiences decline due to a natural mortality rate $d_1$ and predation pressure from cave fish at an interaction rate $b_2$. At the highest trophic level, the fish biomass ($z$) is assumed to be a specialist predator that reproduces solely through the consumption of invertebrates with a conversion efficiency $e_2$, while its biomass decline is determined entirely by the natural mortality rate $d_2$.

Regarding the interaction terms, this model employs a linear functional response (mass-action kinetics) for both consumption levels ($b_1xy$ and $b_2yz$). By defining the state variables as biomass densities, the interaction terms become dimensionally consistent with the rate of change expressed by the differential equations ($mass \cdot area^{-1} \cdot time^{-1}$). This choice is justified by the typically low-density biomass of specialized cave biota, where encounter rates rather than handling time remain the primary limiting factor for energy transfer. Based on the integration of these biological assumptions, the trophic interaction model of the cave ecosystem is formulated as follows:

$$\begin{aligned} \frac{dx}{dt} &= R - b_1xy - ax \\ \frac{dy}{dt} &= b_1e_1xy - b_2yz - d_1y \\ \frac{dz}{dt} &= b_2e_2yz - d_2z \end{aligned} \tag{1}$$

### 2.1. Positivity and Boundedness of Solutions

To ensure the biological validity of the model, it is essential to show that all state variables remain non-negative and bounded for all $t > 0$.

**Theorem 1.** *Solutions $(x(t), y(t), z(t))$ of system (1) with initial conditions in $\mathbb{R}^3_+$ remain in $\mathbb{R}^3_+$ for all $t > 0$.*

*Proof.* From the first equation of system (1), we observe that $\frac{dx}{dt}|_{x=0} = R$. Given that $R > 0$, the guano biomass density $x$ will increase whenever it reaches zero, ensuring $x(t) > 0$. For the biological variables $y$ and $z$, the equations can be expressed as:

$$\frac{dy}{dt} = y(b_1e_1x - b_2z - d_1), \quad \frac{dz}{dt} = z(b_2e_2y - d_2)$$

Integrating these equations yields:

$$y(t) = y(0) \exp\left(\int_0^t (b_1e_1x(\tau) - b_2z(\tau) - d_1)d\tau\right)$$

$$z(t) = z(0) \exp\left(\int_0^t (b_2 e_2 y(\tau) - d_2) d\tau\right)$$

Since the exponential function is strictly positive, $y(t)$ and $z(t)$ will remain positive for all $t > 0$ provided that $y(0) > 0$ and $z(0) > 0$. Thus, the non-negative orthant $\mathbb{R}^3_+$ is an invariant region for the system. □

**Theorem 2.** *All solutions of system (1) initiating in $\mathbb{R}^3_+$ are uniformly bounded.*

*Proof.* Let $W(t) = e_1 e_2 x(t) + e_2 y(t) + z(t)$ be the weighted total biomass of the system. Its time derivative is given by:

$$\begin{aligned}\frac{dW}{dt} &= e_1 e_2 (R - b_1 xy - ax) + e_2 (b_1 e_1 xy - b_2 yz - d_1 y) + (b_2 e_2 yz - d_2 z) \\ &= e_1 e_2 R - e_1 e_2 ax - e_2 d_1 y - d_2 z\end{aligned}$$

Let $\mu = \min(a, d_1, d_2)$ be the minimum decay/mortality rate in the system. We can then establish the following inequality:

$$\frac{dW}{dt} \leq e_1 e_2 R - \mu(e_1 e_2 x + e_2 y + z) = e_1 e_2 R - \mu W$$

Solving this linear differential inequality, we obtain:

$$W(t) \leq \frac{e_1 e_2 R}{\mu} + \left(W(0) - \frac{e_1 e_2 R}{\mu}\right) e^{-\mu t}$$

As $t \to \infty$, it follows that $W(t) \leq \frac{e_1 e_2 R}{\mu}$. Therefore, all solutions starting in $\mathbb{R}^3_+$ are confined within the bounded region $\Omega = \{(x, y, z) \in \mathbb{R}^3_+ : W \leq \frac{e_1 e_2 R}{\mu} + \epsilon\}$ for any $\epsilon > 0$. □

As $t \to \infty$, it follows that $W(t) \leq \frac{e_1 e_2 R}{\mu}$. Therefore, all solutions starting in the positive region are confined within a bounded domain. Having established the fundamental mathematical properties that guarantee the biological feasibility of the model, we proceed to investigate its dynamic behavior through numerical analysis. To ensure the reproducibility of the results and address dimensional clarity, the definitions, parameter values, and units used for the numerical simulations are summarized in Table 1.

While the chosen parameter values are grounded in established ecological literature for cave ecosystems [1, 11, 12], it should be explicitly noted that this parameter set is primarily intended as a theoretical and illustrative example to explore the system's qualitative dynamics, rather than an empirically calibrated case from a specific field site. Given the inherent difficulty in measuring in-situ rates for rare cave biota, this parameter set serves as a biologically realistic baseline to analyze the system's behavior. The sensitivity of the model to these choices is further addressed through the bifurcation analysis, which evaluates how shifts in predation efficiency ($b_2$) influence the overall ecosystem stability.

The analytical methods applied to examine the aforementioned model include qualitative analysis by determining the ecological equilibrium points $(x^*, y^*, z^*)$ under steady-state conditions, where the rate of change of the biomass density over time is zero. Subsequently, stability analysis is performed by constructing the Jacobian matrix to obtain the characteristic equations of the system. The Routh–Hurwitz criteria are utilized to determine the parameter conditions that ensure all eigenvalues have negative real parts, thereby achieving asymptotic stability.

As a final stage, numerical simulation methods are conducted using ODE (Ordinary Differential Equations) integration algorithms in the Python programming language to validate the analytical

**Table 1:** State variables and parameter values with biological justification.

| Symbol | Value | Unit | Biological Justification / Source |
|---|---|---|---|
| *Variables* | | | |
| $x$ | - | mass area$^{-1}$ | Guano biomass density ($g/m^2$). |
| $y$ | - | mass area$^{-1}$ | Invertebrate biomass density ($g/m^2$). |
| $z$ | - | mass area$^{-1}$ | Cave fish biomass density ($g/m^2$). |
| *Parameters* | | | |
| $R$ | 1.5 | mass area$^{-1}$ time$^{-1}$ | Daily guano deposition rate for moderate bat colonies in aphotic cave zones [1]. |
| $a$ | 0.5 | time$^{-1}$ | Microbial decomposition rate of organic matter in high-humidity subterranean environments [11]. |
| $b_1$ | 0.4 | area mass$^{-1}$ time$^{-1}$ | Calibrated consumption rate for detritivores; reflects high search efficiency in nutrient-limited caves [10]. |
| $e_1$ | 0.6 | dimensionless | Trophic efficiency for primary consumers; consistent with high-quality organic subsidies [19]. |
| $d_1$ | 0.2 | time$^{-1}$ | Natural mortality rate for cave invertebrates; estimated for stable, low-fluctuation environments [1]. |
| $b_2$ | 0.3 | area mass$^{-1}$ time$^{-1}$ | Predation rate for specialist fish; assumes encounter-limited dynamics in total darkness (Bifurcation parameter). |
| $e_2$ | 0.7 | dimensionless | High assimilation efficiency typical for specialized top predators in energy-limited systems [19]. |
| $d_2$ | 0.1 | time$^{-1}$ | Low mortality rate reflecting longevity and K-selection strategy of cave-adapted fish [12]. |

results and visualize biomass trajectories within the phase space. Specifically, simulations are implemented using the `scipy.integrate.solve_ivp` library with the RK45 algorithm, employing an absolute tolerance of $10^{-9}$ and a relative tolerance of $10^{-6}$ for numerical precision. Furthermore, the bifurcation analysis is performed using the numerical continuation software `MATCONT` in the MATLAB environment. This procedure employs numerical continuation methods to track equilibrium branches as the predation rate $b_2$ varies, allowing for the precise identification of the Branching Point (BP) and the resulting transcritical bifurcation threshold.

## 3. Results and Discussion

This section presents the analytical and numerical results obtained from the proposed cave ecosystem model. The discussion begins with the equilibrium structure and local stability properties of the system, followed by numerical simulations and bifurcation analysis to illustrate the long-term dynamical behavior of the trophic interactions.

### 3.1. Model Analysis

#### *3.1.1. Equilibrium Points and Existence Analysis*

The equilibrium points of the system (1) are obtained by setting all rates of change with respect to time to zero, $\frac{dx}{dt} = 0$, $\frac{dy}{dt} = 0$, $\frac{dz}{dt} = 0$, such that:

$$\begin{aligned} R - b_1xy - ax &= 0 \\ b_1e_1xy - b_2yz - d_1y &= 0 \\ b_2e_2yz - d_2z &= 0 \end{aligned} \tag{2}$$

Based on the system of equations above, three equilibrium points are obtained along with their existence conditions to remain biologically positive ($x^*, y^*, z^* > 0$):

**1. Equilibrium Point $E_0$.** This point represents the condition where invertebrate biomass density and fish biomass density are absent from the ecosystem ($y^* = 0, z^* = 0$). Substitution into Eq. (2) yields:

$$R - ax = 0 \implies x_0^* = \frac{R}{a} \tag{3}$$

Thus, the equilibrium point is obtained:

$$E_0 = \left(\frac{R}{a}, 0, 0\right) \tag{4}$$

Biological existence condition for $E_0$: Since the parameters $R$ (input rate) and $a$ (decomposition rate) are always positive ($R, a > 0$), $x_0^* > 0$ is always satisfied. The point $E_0$ always exists under any parameter conditions.

**2. Equilibrium Point $E_1$.** This point represents the existence of guano and invertebrate biomass densities in the absence of fish ($x^*, y^* > 0, z^* = 0$). From Eq. (2), we obtain:

$$y(b_1 e_1 x - d_1) = 0 \tag{5}$$

Since $y > 0$, it must follow that $b_1 e_1 x - d_1 = 0$, hence:

$$x_1^* = \frac{d_1}{b_1 e_1} \tag{6}$$

Substituting the value of $x_1^*$ into Eq. (2) to solve for $y_1^*$:

$$\begin{aligned} R - b_1\left(\frac{d_1}{b_1 e_1}\right) y - a\left(\frac{d_1}{b_1 e_1}\right) &= 0 \\ \frac{d_1}{e_1} y &= R - \frac{a d_1}{b_1 e_1} \\ y_1^* = \frac{e_1}{d_1}\left(\frac{R b_1 e_1 - a d_1}{b_1 e_1}\right) &= \frac{R b_1 e_1 - a d_1}{b_1 d_1} \end{aligned}$$

Thus, the equilibrium point is obtained:

$$E_1 = \left(\frac{d_1}{b_1 e_1}, \frac{R b_1 e_1 - a d_1}{b_1 d_1}, 0\right) \tag{7}$$

Existence condition for $E_1$:

$$\begin{aligned} & d_1, e_1, b_1 > 0 \\ R b_1 e_1 - a d_1 > 0 \implies & R b_1 e_1 > a d_1 \end{aligned} \tag{8}$$

**3. Coexistence Equilibrium Point ($E_2$).** This point represents the condition where all three components (guano, invertebrate, and fish biomass densities) coexist ($x^*, y^*, z^* > 0$). From Eq. (2), we obtain:

$$z(b_2 e_2 y - d_2) = 0 \implies y_2^* = \frac{d_2}{b_2 e_2} \tag{9}$$

Substituting $y_2^*$ into the equation to obtain $x_2^*$:

$$\begin{aligned} R - b_1 x\left(\frac{d_2}{b_2 e_2}\right) - ax &= 0 \\ x\left(\frac{b_1 d_2 + a b_2 e_2}{b_2 e_2}\right) = R \implies x_2^* &= \frac{R b_2 e_2}{b_1 d_2 + a b_2 e_2} \end{aligned}$$

Next, substituting $x_2^*$ into the equation to obtain $z_2^*$:

$$b_1e_1x_2^*y_2^* - b_2y_2^*z - d_1y_2^* = 0$$
$$b_1e_1x_2^* - b_2z - d_1 = 0 \implies z_2^* = \frac{b_1e_1x_2^* - d_1}{b_2}$$

Thus, the interior equilibrium point is obtained:

$$E_2 = \left(\frac{Rb_2e_2}{b_1d_2 + ab_2e_2}, \frac{d_2}{b_2e_2}, \frac{b_1e_1x_2^* - d_1}{b_2}\right) \tag{10}$$

Existence condition for $E_2$: The point $E_2$ exists if $x_2^* > 0$, $y_2^* > 0$, $z_2^* > 0$. This requires:

$$b_1e_1x_2^* > d_1 \implies x_2^* > \frac{d_1}{b_1e_1} \tag{11}$$

By substituting the value of $x_2^*$, this condition becomes:

$$\frac{Rb_1e_1b_2e_2}{b_1d_2 + ab_2e_2} > d_1 \implies R > \frac{d_1(b_1d_2 + ab_2e_2)}{b_1e_1b_2e_2} \tag{12}$$

$$Rb_1e_1b_2e_2 > d_1(b_1d_2 + ab_2e_2) \tag{13}$$

*3.1.2. Stability Analysis*

To analyze the dynamic behavior of system (1) around the equilibrium points, linearization is performed using the Jacobian matrix $J(x, y, z)$. The Jacobian matrix of the system is defined as follows:

$$J(x, y, z) = \begin{bmatrix} -b_1y - a & -b_1x & 0 \\ b_1e_1y & b_1e_1x - b_2z - d_1 & -b_2y \\ 0 & b_2e_2z & b_2e_2y - d_2 \end{bmatrix} \tag{14}$$

Local stability is determined by the eigenvalues ($\lambda$) of the characteristic equation $|J(E_i) - \lambda I| = 0$. An equilibrium point is locally asymptotically stable if all eigenvalues have negative real parts ($Re(\lambda_i) < 0$).

**Theorem 3.** *The equilibrium point $E_0$ is locally asymptotically stable if the condition $\frac{R}{a} < \frac{d_1}{b_1e_1}$ is satisfied.*

*Proof.* Evaluating the Jacobian matrix at $E_0 = (\frac{R}{a}, 0, 0)$ yields:

$$J(E_0) = \begin{bmatrix} -a & -\frac{b_1R}{a} & 0 \\ 0 & \frac{b_1e_1R}{a} - d_1 & 0 \\ 0 & 0 & -d_2 \end{bmatrix} \tag{15}$$

The characteristic equation of $J(E_0)$ is $(-a - \lambda)(\frac{b_1e_1R}{a} - d_1 - \lambda)(-d_2 - \lambda) = 0$. The eigenvalues are obtained directly from the diagonal elements: $\lambda_1 = -a$, $\lambda_2 = \frac{b_1e_1R}{a} - d_1$, and $\lambda_3 = -d_2$. Since $a, d_2 > 0$, then $\lambda_1, \lambda_3 < 0$. For $\lambda_2 < 0$, it must hold that $\frac{b_1e_1R}{a} < d_1$, or equivalently $\frac{R}{a} < \frac{d_1}{b_1e_1}$. □

**Theorem 4.** *The equilibrium point $E_1$ is locally asymptotically stable if the condition $y_1^* < \frac{d_2}{b_2e_2}$ is satisfied.*

*Proof.* At the point $E_1 = (x_1^*, y_1^*, 0)$, the equilibrium condition implies $b_1 e_1 x_1^* - d_1 = 0$. The Jacobian matrix evaluated at $E_1$ is:

$$J(E_1) = \begin{bmatrix} -(b_1 y_1^* + a) & -b_1 x_1^* & 0 \\ b_1 e_1 y_1^* & 0 & -b_2 y_1^* \\ 0 & 0 & b_2 e_2 y_1^* - d_2 \end{bmatrix} \tag{16}$$

The characteristic equation is obtained by solving $|J(E_1) - \lambda I| = 0$. Using cofactor expansion along the third row, we obtain:

$$(b_2 e_2 y_1^* - d_2 - \lambda) \det \left( \begin{bmatrix} -(b_1 y_1^* + a) - \lambda & -b_1 x_1^* \\ b_1 e_1 y_1^* & -\lambda \end{bmatrix} \right) = 0 \tag{17}$$

The first eigenvalue is $\lambda_3 = b_2 e_2 y_1^* - d_2$, which is negative if $y_1^* < \frac{d_2}{b_2 e_2}$. The remaining two eigenvalues, $\lambda_{1,2}$, are determined by the $2 \times 2$ upper-left submatrix $J_{sub}$. For this submatrix, the trace (Tr) and determinant (Det) are computed as follows:

$$\begin{aligned} \mathrm{Tr}(J_{sub}) &= -(b_1 y_1^* + a) + 0 = -(b_1 y_1^* + a) \\ \mathrm{Det}(J_{sub}) &= (-(b_1 y_1^* + a))(0) - (-b_1 x_1^*)(b_1 e_1 y_1^*) = b_1^2 e_1 x_1^* y_1^* \end{aligned} \tag{18}$$

The characteristic polynomial for these eigenvalues is $P(\lambda) = \lambda^2 - \mathrm{Tr}(J_{sub})\lambda + \mathrm{Det}(J_{sub}) = 0$, which can be written as $P(\lambda) = \lambda^2 + A_1 \lambda + A_2 = 0$, where:

$$A_1 = b_1 y_1^* + a, \quad A_2 = b_1^2 e_1 x_1^* y_1^* \tag{19}$$

According to the Routh–Hurwitz criteria, for $\lambda_{1,2}$ to have negative real parts, the coefficients must satisfy $A_1 > 0$ and $A_2 > 0$. Since all parameters and equilibrium biomass densities are positive, these conditions are inherently satisfied, concluding the proof. □

**Theorem 5.** *The coexistence equilibrium point $E_2$ is locally asymptotically stable throughout its existence domain.*

*Proof.* At the point $E_2 = (x^*, y^*, z^*)$, the equalities $b_1 e_1 x^* - b_2 z^* - d_1 = 0$ and $b_2 e_2 y^* - d_2 = 0$ hold. The Jacobian matrix $J(E_2)$ becomes:

$$J(E_2) = \begin{bmatrix} -(b_1 y^* + a) & -b_1 x^* & 0 \\ b_1 e_1 y^* & 0 & -b_2 y^* \\ 0 & b_2 e_2 z^* & 0 \end{bmatrix} \tag{20}$$

The characteristic equation $|J(E_2) - \lambda I| = 0$ is $\lambda^3 + A\lambda^2 + B\lambda + C = 0$, with coefficients:

$$\begin{aligned} A &= b_1 y^* + a \\ B &= b_2^2 e_2 y^* z^* + b_1^2 e_1 x^* y^* \\ C &= (b_1 y^* + a)(b_2^2 e_2 y^* z^*) \end{aligned}$$

According to the Routh–Hurwitz criteria, the system is stable if $A > 0, C > 0$, and $AB > C$. The conditions $A, C > 0$ are satisfied trivially. Calculating $AB - C$ yields:

$$\begin{aligned} AB - C &= (b_1 y^* + a)(b_2^2 e_2 y^* z^* + b_1^2 e_1 x^* y^*) - (b_1 y^* + a)(b_2^2 e_2 y^* z^*) \\ &= (b_1 y^* + a)[(b_2^2 e_2 y^* z^* + b_1^2 e_1 x^* y^*) - b_2^2 e_2 y^* z^*] \\ &= (b_1 y^* + a)(b_1^2 e_1 x^* y^*) \end{aligned}$$

Since $a, b_1, e_1, x^*, y^* > 0$, then $AB - C > 0$ is always satisfied. Consequently, the coexistence point $E_2$ is always locally asymptotically stable as long as the biomass densities at the equilibrium are biologically existent ($z^* > 0$). □

## 3.2. Numerical Simulation

### *3.2.1. Phase Portrait*

The verification of the interaction dynamics between guano biomass density ($x$), the invertebrate biomass density ($y$), and the fish biomass density ($z$) was conducted through numerical simulations using the Python programming language, utilizing the `solve_ivp` function from the `SciPy` library. The integration of this system of non-linear differential equations was solved using the Runge-Kutta order 4(5) algorithm or the *Explicit Runge-Kutta method of order 5(4)* (RK45) over a simulation time range of $t \in [0, 200]$, with an evaluation resolution of 1500 data points to ensure the accuracy of the solution trajectories.

The parameter values were established based on assumptions that satisfy the existence and asymptotic stability criteria of the coexistence point, namely $a = 0.5$, $b_1 = 0.4$, $b_2 = 0.3$, $e_1 = 0.6$, $e_2 = 0.7$, $d_1 = 0.2$, $d_2 = 0.1$, and $R = 1.5$. Based on these assumed parameters, the system generates three equilibrium points representing the biomass hierarchy: the consumer-free point $E_0(3.0, 0, 0)$, the predator-free point $E_1(0.833, 3.25, 0)$, and the interior or coexistence point $E_2(2.172, 0.476, 1.071)$. The condition $E_0$ reflects an environmental status dominated solely by the biomass density of guano nutrients without the presence of consumers, while $E_1$ indicates the inability of the fish biomass density to establish itself in the ecosystem despite an abundant supply of invertebrates as a food source under this specific numerical configuration.

Stability analysis at the interior point $E_2$ yielded an eigenvalue $\lambda_1 = -0.519706$ and a pair of complex conjugates $\lambda_{2,3} = -0.085385 \pm 0.188169j$. The presence of real parts that are entirely negative mathematically confirms that the coexistence point $E_2$ is locally asymptotically stable with the characteristics of a stable focus within the local vicinity of the equilibrium. Biologically, the negative real eigenvalue ($\lambda_1$) represents the ecosystem's theoretical resilience in balancing the guano input rate as the primary nutrient base, ensuring its availability remains controlled despite external disturbances. The presence of the complex conjugate pair ($\lambda_{2,3}$) reflects dynamic predation dynamics, where the invertebrate and fish biomass densities undergo damped fluctuations before eventually reaching a constant biomass density. This phenomenon indicates that under the chosen parameter set, the nutrient input rate from guano ($R$) and the efficiency of energy transfer between trophic levels allow for a steady state where the invertebrate biomass density persists despite predation pressure.

The system dynamics were further tested through five initial condition (IC) variations representing various scenarios of initial biomass densities within the phase space $\mathbb{R}^3_+$, specifically $IC_1(0.5, 0.2, 0.1)$, $IC_2(3.0, 1.0, 0.5)$, $IC_3(1.0, 2.0, 1.5)$, $IC_4(4.0, 0.5, 0.2)$, and $IC_5(2.5, 1.5, 0.8)$.

As visualized in the three-dimensional phase portrait in Fig. 1, all trajectories originating from various starting points move dynamically and converge toward the equilibrium point $E_2$. The spiral patterns in the paths toward the central point are physical manifestations of biomass adaptation to nutrient availability and predation pressures that stabilize one another within the modeled framework. These results suggest that for this specific numerical configuration, the system exhibits a balancing mechanism where biomass densities converge toward coexistence. Conversely, points $E_0$ and $E_1$ are unstable, implying that the system tends to move away from extinction states and toward the stable coexistence point $E_2$ for the given parameter values.

### *3.2.2. Time Series with Different Initial Conditions*

To understand the dynamic behavior of the guano–invertebrate–fish interaction model, numerical simulations of the nonlinear differential equation system were conducted using the numerical integration methods available in the `solve_ivp` function of the *SciPy* library in the Python

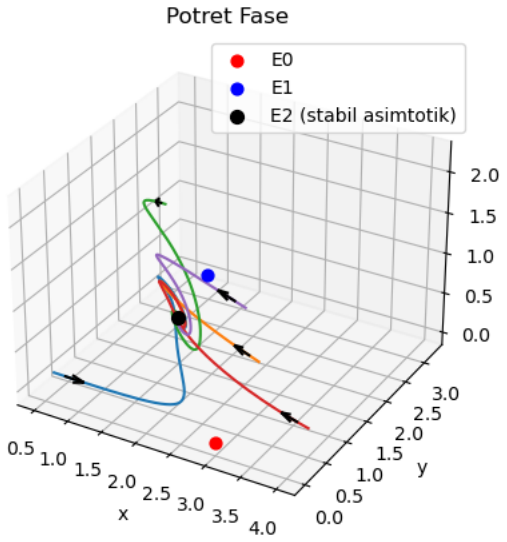


**Fig. 1:** 3D phase portrait of the guano-invertebrate-fish model showing the convergence of trajectories from five initial conditions toward the coexistence equilibrium point $E_2$.

programming language. By default, this function employs the adaptive Runge–Kutta order 4–5 (RK45) method, which is capable of producing stable and accurate numerical solutions.

Simulations were performed over the time interval $t \in [0, 200]$ with 2000 evaluation points, allowing the biomass dynamics to be observed in detail over time. In this model, the variable $x(t)$ represents the biomass density of guano as a nutrient source, $y(t)$ denotes the invertebrate biomass density as primary consumers, and $z(t)$ denotes the fish biomass density as predators. To test the system's stability against variations in initial conditions, several simulations were conducted with different initial biomass values.

While the previous phase portrait illustrated the qualitative convergence of the system from various points in the phase space, the following simulations employ a specific set of initial conditions to examine the detailed transient oscillations and the temporal adaptation of each biomass density toward the steady state.

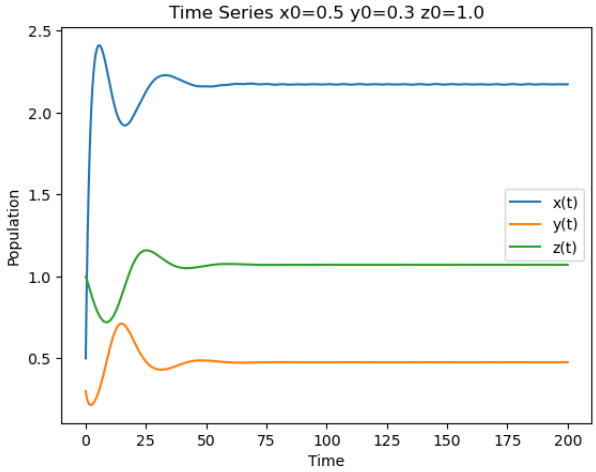


**Fig. 2:** Time series simulation of the guano–invertebrate–fish model with initial conditions $x_0 = 0.5$, $y_0 = 0.3$, and $z_0 = 1.0$.

**Simulation 1: Initial Conditions $x_0 = 0.5$, $y_0 = 0.3$, $z_0 = 1.0$.** In the first simulation, the initial fish biomass density is relatively larger than the invertebrate biomass density. The simulation

results show that the guano biomass density $x(t)$ initially increases rapidly due to the external nutrient supply $R$. However, as the invertebrate biomass density which utilizes guano as a food source increases, the growth rate of the guano begins to decrease until it eventually approaches the equilibrium value $E_2$ at the point $x = 2.172$.

The invertebrate biomass density $y(t)$ exhibits oscillatory dynamics in the early stages caused by the interaction between growth due to nutrient availability and decline due to fish predation. The amplitude of these oscillations gradually diminishes until the biomass density finally reaches a stable state at the point 0.476. Meanwhile, the fish biomass density $z(t)$ experiences a slight initial decline before increasing again as the prey biomass grows. After undergoing several damped oscillations, the entire biomass density converges toward the equilibrium state at the point 1.071.

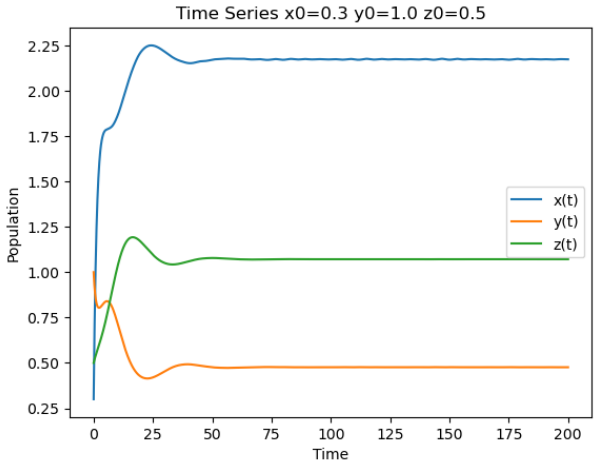


**Fig. 3:** Time series simulation of the guano–invertebrate–fish model with initial conditions $x_0 = 0.3$, $y_0 = 1.0$, and $z_0 = 0.5$.

**Simulation 2: Initial Conditions $x_0 = 0.3$, $y_0 = 1.0$, $z_0 = 0.5$.** In the second simulation, the initial invertebrate biomass density is higher than the other biomass densities. This condition leads to more intensive guano consumption in the initial stage. Nevertheless, due to the constant guano supply from the environment, the guano biomass density continues to increase gradually until it nears the same $E_2$ equilibrium value as in the first simulation, at $x = 2.172$.

The invertebrate biomass density declines after the initial phase due to predation pressure from the fish. Subsequently, the system exhibits small oscillations that gradually subside before the biomass density reaches a stable state. The fish biomass density initially increases in response to the high availability of prey, but its growth slows down as the prey biomass density begins to decrease toward equilibrium.

**Simulation 3: Initial Conditions $x_0 = 1.0$, $y_0 = 0.5$, $z_0 = 0.3$.** In the third simulation, the guano biomass density has a relatively higher initial value while the fish biomass density is relatively lower. This condition causes the invertebrate biomass density to increase quite rapidly in the initial stage due to the abundant nutrient source and relatively low predation pressure. Over time, the increase in the invertebrate biomass density triggers the growth of the fish biomass density. The predator-prey interaction produces transient oscillations across all three biomass densities before they eventually subside. After passing through this transient phase, all biomass densities return to the same $E_2$ equilibrium value as in the previous dua simulations.

The three simulations with different initial conditions demonstrate that for the specific parameter set assumed, all system solutions eventually converge toward the same equilibrium point, $E_2(2.172, 0.476, 1.071)$, after undergoing a transient phase of diminishing oscillations. This

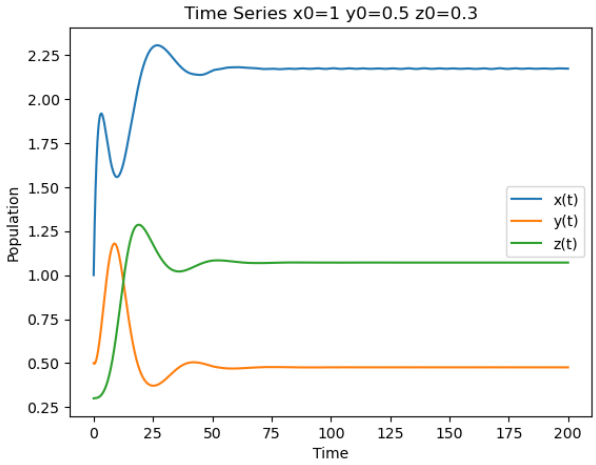


**Fig. 4:** Time series simulation of the guano–invertebrate–fish model with initial conditions $x_0 = 1.0$, $y_0 = 0.5$, and $z_0 = 0.3$.

numerically suggests that the interior equilibrium point of the model is asymptotically stable within the tested range. Thus, the modeled system exhibits the theoretical capability to return to a stable state despite variations in initial biomass conditions.

Biologically, these results suggest that within the framework of this model, the trophic interactions between guano as the basal nutrient source, invertebrates as primary consumers, and fish as predators can potentially form a stable configuration. The continuous guano supply plays a vital role in supporting the food chain, while predatory interactions help regulate biomass growth, suggesting a potential for maintaining ecological balance under the idealized conditions represented by the chosen parameters.

### 3.3. Bifurcation

To further investigate the sensitivity of the ecosystem stability toward changes in predation efficiency, a bifurcation analysis was performed using the predation rate of cave fish ($b_2$) as the primary bifurcation parameter. The equilibrium branches were numerically traced using the `MATCONT` continuation package in the MATLAB environment, which utilizes numerical continuation methods to detect stability switches by monitoring the system's eigenvalues along the computed curves.

While the critical transition point is identified numerically, it is fundamentally rooted in the analytical stability conditions of the predator-free equilibrium $E_1(x_1^*, y_1^*, 0)$. According to Theorem 2, the point $E_1$ loses its stability when the eigenvalue $\lambda_3 = b_2 e_2 y_1^* - d_2$ crosses zero. By setting $\lambda_3 = 0$, we can derive the exact analytical expression for the transcritical bifurcation threshold ($b_2^*$):

$$b_2^* = \frac{d_2}{e_2 y_1^*} \tag{21}$$

where $y_1^*$ is the steady-state invertebrate biomass density at the predator-free equilibrium. By substituting the parameter values consistent with the simulation results ($d_2 = 0.1$, $e_2 = 0.7$, and $y_1^* = 3.25$) into Eq. (21), we obtain:

$$b_2^* = \frac{0.1}{0.7 \times 3.25} \approx 0.043956$$

This analytical result is now perfectly consistent with the numerical continuation results. The analysis identifies a critical transition point known as a Branching Point (BP), as illustrated in Fig. 5. The numerical results indicate that the Branching Point occurs at the following coordinates:

$$BP : (x, y, z; b_2) = (0.833333, 3.250000, 0.000000; 0.043956) \tag{22}$$

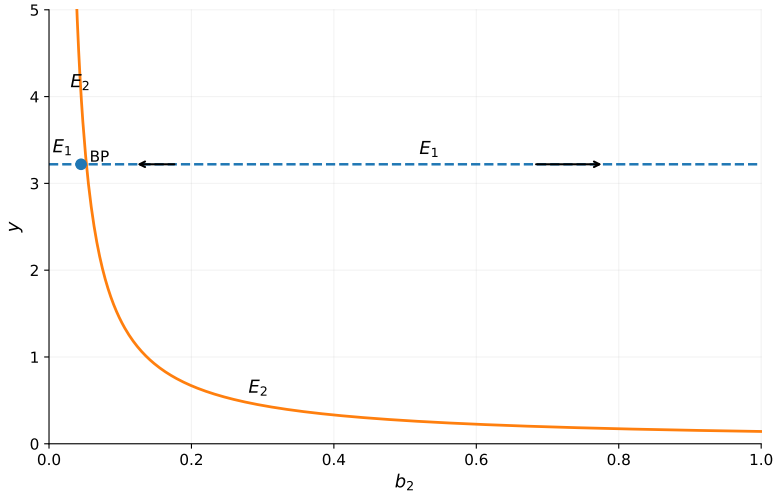


**Fig. 5:** Bifurcation diagram of invertebrate biomass density ($y$) against the predation rate ($b_2$). The solid line represents stable equilibrium, while the dashed line represents unstable equilibrium.

The bifurcation diagram reveals a Transcritical Bifurcation at $b_2^* \approx 0.043956$. Biologically, within the scope of this model, this point represents the predator invasion threshold. The dynamics can be categorized into two distinct ecological regimes under the assumed parameter set:

1. **Predator-Extinction Regime ($b_2 < 0.043956$):** When the predation rate is below this threshold, the cave fish cannot efficiently extract enough energy from the invertebrate biomass density to compensate for their natural mortality rate ($d_2 = 0.1$). In this regime, the predator-free equilibrium $E_1$ (represented by the horizontal line at $y = 3.25$) is stable. The fish biomass ($z$) inevitably converges to zero.
2. **Coexistence Regime ($b_2 > 0.043956$):** As $b_2$ crosses the critical value $b_2^*$, the predator-free equilibrium loses its stability (indicated by the transition to a dashed line), and a new stable branch $E_2$ emerges. This signifies that the fish biomass can theoretically successfully colonize the cave. As the predation efficiency $b_2$ increases, the steady-state biomass density of invertebrates ($y$) follows a non-linear decay curve, demonstrating a potential top-down control mechanism.

The existence of the BP highlights the theoretical fragility of specialized cave biota under these idealized conditions. If environmental changes reduce the fish's ability to hunt ($b_2$), the system may cross the BP in reverse, leading to the collapse of the predator level and a subsequent boom in the invertebrate biomass density. This analysis suggests that the mathematical stability of the cave's food web is fundamentally bounded by a minimum threshold of energy transfer efficiency ($b_2^*$) between the primary consumers and top predators.

## 4. Conclusion

This research investigated the interaction dynamics between guano biomass density ($x$), invertebrate biomass density ($y$), and fish biomass density ($z$) through a three-compartment trophic model representing a semi-closed cave ecosystem. The analytical results identified three primary equilibrium points: the consumer-free point $E_0$, the predator-free point $E_1$, and the coexistence point $E_2(2.172, 0.476, 1.071)$. Local stability analysis at $E_2$ yielded eigenvalues of $\lambda_1 = -0.519706$ and $\lambda_{2,3} = -0.085385 \pm 0.188169i$, which mathematically confirms that the coexistence point is locally asymptotically stable with the characteristics of a stable focus under the conditions analyzed. These results indicate that within the specific numerical configuration of the model, all three biomass densities can maintain a stable state of coexistence.

Furthermore, the bifurcation analysis revealed a critical Branching Point (BP) at the predation rate $b_2 \approx 0.043956$, which was supported by both numerical continuation via `MATCONT` and analytical derivation. This point signifies a theoretical threshold for predator invasion; below this value, the fish biomass fails to persist, leading to a predator-free environment. Crossing this threshold triggers a transcritical bifurcation that potentially allows for a stable coexistence regime, where the predator exerts a significant top-down control on the invertebrate biomass density. The discovery of this BP highlights the mathematical sensitivity of the cave's food web to the efficiency of energy transfer between trophic levels.

Numerical simulations using the Runge–Kutta order 4(5) method via the `solve_ivp` function in the `SciPy` library support the theoretical findings. Time-series simulations exhibited damped oscillations before the biomass densities reached a steady state, while the three-dimensional phase portrait demonstrated that trajectories from various initial conditions converge toward the coexistence point $E_2$. While these findings suggest a potential for ecological balance through top-down control and nutrient-dependent dynamics, it should be emphasized that these conclusions are strictly based on local stability analysis and assumed parameter values rather than empirical validation.

As a theoretical study, a primary limitation is the absence of direct calibration with field data, and the specific codes used for ini simulations are not publicly available. Future research could enhance this model by incorporating more realistic functional responses, seasonal variations in guano supply, or the influence of stochastic environmental fluctuations. Despite these limitations, this model provides a fundamental theoretical framework for understanding the energy-limited trophic dynamics of guano-based cave ecosystems under idealized conditions.

## CRediT Authorship Contribution Statement

**M. Niko Axsella Ibrahim:** Conceptualization, Methodology, Software, Formal Analysis, Investigation, Writing–Original Draft, Visualization. **Dian Savitri:** Conceptualization, Methodology, Validation, Writing–Review & Editing, Visualization, Supervision.

## Declaration of Generative AI and AI-assisted technologies

No generative AI or AI-assisted technologies were used during the preparation of this manuscript.

## Declaration of Competing Interest

The authors declare no competing interests.

## Funding and Acknowledgments

The authors wish to extend their deepest gratitude to their supervisor for the profound mentorship, unwavering encouragement, and critical insights provided throughout the progression of this research. Furthermore, sincere appreciation is expressed to all colleagues and individuals whose technical expertise and collective support were instrumental in the successful completion of this manuscript.

## Data and Code Availability

data and code not available.

## References

[1] David C. Culver and Tanja Pipan. *The Biology of Caves and Other Subterranean Habitats*. 2nd. Oxford University Press, 2019. DOI: 10.1093/oso/9780198820765.001.0001.

[2] Oana Teodora Moldovan, Lubomir Kovac, and Stuart Halse. *Cave Ecology*. Springer Cham, 2018. DOI: 10.1007/978-3-319-98852-8.

[3] Gary A. Polis, Stephen D. Hurd, C. T. Jackson, and Francisco Sanchez-Pinero. "Toward an Integration of Landscape Ecology and Food Web Ecology: The Dynamics of Spatially Subsidized Food Webs". In: *Annual Review of Ecology and Systematics* 28 (1997), pp. 289–316. DOI: 10.1146/annurev.ecolsys.28.1.289.

[4] Boris Sket. "The nature of biodiversity in hypogean waters and how it is endangered". In: *Biodiversity and Conservation* 8.10 (1999), pp. 1319–1338. DOI: 10.1023/A:1008916601121.

[5] Mohammed Kasso and Mundanthra Balakrishnan. "Ecological and Economic Importance of Bats (Order Chiroptera)". In: *ISRN Biodiversity* 2013 (2013), pp. 1–9. DOI: 10.1155/2013/187415.

[6] Rodrigo L. Ferreira and Rogerio P. Martins. "Trophic structure and natural history of bat guano invertebrate communities, with special reference to Brazilian caves". In: *Tropical Zoology* 12.2 (1999), pp. 231–252. DOI: 10.1080/03946975.1999.10539391.

[7] Angel Garcia-Bodelon, Najla Bakovic, Emilio Cano, Fernando Useros, Enrique Lara, and Ruben Gonzalez-Miguens. "Predators in the Dark: Metabarcoding Reveals Arcellinida Communities Associated with Bat Guano, Endemic to Dinaric Karst in Croatia". In: *Microbial Ecology* 87.1 (2024), p. 166. DOI: 10.1007/s00248-024-02483-z.

[8] Christopher M. Wurster, Niels Munksgaard, and Michael I. Bird. "Bat guano isotope systems integrate environmental, climatic, and ecological signals". In: *Quaternary Science Reviews* 334 (2024), p. 108711. DOI: 10.1016/j.quascirev.2024.108711.

[9] Valentina Balestra, Rossana Bellopede, and Stefano Mammola. "Macroinvertebrate diversity patterns in a guano-rich temperate cave". In: *bioRxiv* (2025). DOI: 10.1101/2025.02.09.637321.

[10] Andrea Parimuchová, Lenka Petráková Dušátková, Ľubomír Kováč, Táňa Macháčková, Ondřej Slabý, and Stano Pekár. "The food web in a subterranean ecosystem is driven by intraguild predation". In: *Scientific Reports* 11.1 (2021), p. 4994. DOI: 10.1038/s41598-021-84521-1.

[11] Nynne Marie Rand Ravn, Anders Michelsen, and Ana Sofia P. S. Reboleira. "Decomposition of Organic Matter in Caves". In: *Frontiers in Ecology and Evolution* 8 (2020), p. 554651. DOI: 10.3389/fevo.2020.554651.

[12] Veronica Nanni, Elena Piano, Pedro Cardoso, Marco Isaia, and Stefano Mammola. "An expert-based global assessment of threats and conservation measures for subterranean ecosystems". In: *Biological Conservation* 283 (2023), p. 110136. DOI: 10.1016/j.biocon.2023.110136.

[13] Andrea Castaño-Sánchez, Grant C. Hose, and Ana Sofia P. S. Reboleira. "Ecotoxicological effects of anthropogenic stressors in subterranean organisms: A review". In: *Chemosphere* 244 (2020), p. 125422. DOI: 10.1016/j.chemosphere.2019.125422.

[14] Julio David Soto-Lopez et al. "Taxonomic and functional profiling of bat guano microbiota from hiking trail-associated tunnels: a potential risk for human health?" In: *Environmental Microbiome* 20.1 (2025), p. 123. DOI: 10.1186/s40793-025-00782-7.

[15] Alan Hastings and Thomas Powell. "Chaos in a three-species food chain". In: *Ecology* 72.3 (1991), pp. 896–903. DOI: 10.2307/1940591.

[16] Mihaela Sterpu, Carmen Rocşoreanu, Raluca Efrem, and Sue Ann Campbell. "Stability and Bifurcations in a Nutrient–Phytoplankton–Zooplankton Model with Delayed Nutrient Recycling with Gamma Distribution". In: *Mathematics* 11.13 (2023), p. 2911. DOI: 10.3390/math11132911.

[17] Wenjie Yang, Qianqian Zheng, Jianwei Shen, and Linan Guan. "Bifurcation and pattern dynamics in the nutrient-plankton network". In: *Mathematical Biosciences and Engineering* 20.12 (2023), pp. 21337–21358. DOI: 10.3934/mbe.2023944.

[18] Jose Luiz Attayde and Jörgen Ripa. "The coupling between grazing and detritus food chains and the strength of trophic cascades across a gradient of nutrient enrichment". In: *Ecosystems* 11.6 (2008), pp. 980–990. DOI: 10.1007/s10021-008-9174-8.

[19] Raymond L. Lindeman. "The Trophic-Dynamic Aspect of Ecology". In: *Ecology* 23.4 (1942), pp. 399–417. DOI: 10.2307/1930126.